



Research on polymer solution rheology in polymer flooding for Qikou reservoirs in a Bohai Bay oilfield

Leilei Tie¹ · Meng Yu¹ · Xiang Li¹ · Wenhui Liu¹ · Bo Zhang¹ · Zhen Chang¹ · Yufei Zheng¹

Received: 27 December 2017 / Accepted: 4 July 2018 / Published online: 13 July 2018
© The Author(s) 2018

Abstract

This study explored the potential applications of three newly modified polymers [a linear polymer, a hydrophobic association of partially hydrolyzed polyacrylamide (HAHPAM), and a polymer–surfactant] as flooding agents in a specific oilfield. Rheological measurements were performed to examine the rheological performances of the three polymers under reservoir conditions. Their stability, viscoelasticity, and propagation properties were analyzed under simulated reservoir conditions. Propagation performance analyses were conducted in a sandpack model to study the propagation behavior of the three polymers in porous media. The results of the rheological study showed that the HAHPAM and polymer–surfactant exhibited high viscosity at low shear rates (deep reservoir), and all three showed acceptable viscosity with good injectivity at high shear rates (near wellbore area). In oscillatory deformation tests, the HAHPAM and polymer–surfactant showed a predominantly elastic behavior. The results of the propagation performance showed the linear polymer and polymer–surfactant could propagate well in porous media, whereas the HAHPAM showed poor propagation behavior. This finding contrasted with rheological tests in which the injectivity of HAHPAM was superior, with high viscosity at low shear rates. The results of the study provided insights either into matching the viscoelastic performance with propagation behavior in porous media, or upon analyzing the suitability of the polymers for flooding throughout a whole process under “from injectivity to propagation” considerations.

Keywords Profile control · Linear polymer · Polymer–surfactant hydrophobically associating polyacrylamide · Rheological properties · Propagation properties

List of symbols

r The average pore radius (m)
 k Formation permeability (m^2)

ϕ Porosity
 $\dot{\gamma}$ Shear rate (s^{-1})
 δ Coefficient of correction, a parameter that was found to be equal to 2.5 for particles of angular shapes
 v Superficial velocity ($m\ day^{-1}$)
 T Experimental temperature ($^{\circ}C$)
 η Apparent viscosity ($mPa\ s$)
 η_0 Zero shear rate viscosity
 λ Relaxation time
 K Consistency coefficient ($Pa\ s$)
 n The flow behavior index
 R Correlation coefficient
 G' Elastic modulus (Pa)
 G'' Viscous modulus (Pa)
 C_p Polymer concentration, ppm ($mg\ L^{-1}$)
 r_p Molecular cyclotron radius (μm)
 r_h Pore throat radius (μm)

✉ Leilei Tie
tieleilei@126.com
Meng Yu
ymshida@126.com
Xiang Li
lixiang20@cosl.com.cn
Wenhui Liu
liuwh11@cosl.com.cn
Bo Zhang
zhangbo21@cosl.com.cn
Zhen Chang
changzhen@cosl.com.cn
Yufei Zheng
zhengyf4@cosl.com.cn

¹ Application and Research Center, Oilfield Production Optimization, China Oilfield Services Limited, CNOOC, Tianjin 300459, People's Republic of China

Introduction

Among the diverse enhanced oil recovery strategies, such as water flooding and gas flooding, polymer flooding is a preferable option for many oilfields. When accounting for the regional reservoir conditions of offshore Bohai Bay oilfields, polymer flooding is a more favorable chemical EOR method compared to waterflooding.

During the polymer flooding process, a given amount of a high molecular weight polymer is added to the displacing phase to improve its viscosity and thus produce a promising mobility condition (Alvarado and Manrique 2010; Silva et al. 2007; Chang et al. 2006). Standnes, DC summarized the implemented polymer injection projects on a pilot or field scale mentioned in the literature over the last 50 years. The primary reasons explaining the technically discouraging cases were found to be low permeability, low injected polymer concentration, high viscosity reduction, poor injectivity, very high permeability contrast and extremely high polymer retention (Standnes and Skjevrak 2014). Saboorian-Jooybari et al. (2015, 2016) reviewed the advances and technological trends in polymer flooding of heavy oil reservoirs since the 1960s, and they developed new screening criteria for heavy oil reservoirs according to an analysis of the data. Delamaide discussed many aspects of polymer flooding in heavy oil reservoirs, including reservoir and surface issues, and he provided guidelines and screening criteria for the entire process. He concluded that despite the existing challenges, such as oil viscosity and oil–water separation, the polymer flooding of heavy oils could result in incremental recoveries ranging from 7.5 to 25% OOIP (Delamaide 2014). Seright showed a detailed discussion of two important questions in polymer flooding. One is the polymer solution viscosity that should be injected, and a base-case reservoir-engineering method was presented to decide the polymer solution viscosity. He advised that high polymer viscosities be favored over low polymer viscosities when considering reservoir heterogeneity and economic factors, if the injectivity is not limiting. The other is when the polymer injection should be stopped or reduced. Based on technical and economic considerations, this time depended greatly on the oil price, polymer cost, and many individual factors associated with a given field (Seright and April 2016).

The viscoelastic properties of a displacement fluid are known to have a significant effect on the oil displacement efficiency in a chemical EOR process. As early as 1970, Smith (1970) and Acharya (1986) mentioned that polymer solutions exhibited viscoelastic properties in porous media. When the viscosity of the polymer is too high at the injection period, it may result in worse injectivity and propagation performance, easily blocking the oil-producing layer.

However, if the viscosity of the injected fluid is too low, the propagation performance of the polymer solutions can be improved, but the low viscosity can hardly fulfill the requirement for mobility control (Cheng et al. 2000). This challenge may affect the economic benefits of polymer flooding. Therefore, before planning to perform polymer flooding in oilfields, it is critical to understand the relationship between the polymer rheological behaviors of the designed polymer concentration and its adaptability to reservoir conditions. Ghoumrassi-Barr conducted studies on the feasibility of polymer flooding in a specific field according to an elaborate analysis of rheological properties in the tested polymer solutions (Sofia and Djamel 2016). Numerous rheological tests, such as dynamic viscoelastic and steady flow measurements, were performed under various polymer concentrations, salinities, reservoir temperatures, and storage times. Xia conducted a study to investigate the effects of non-Newtonian-displacing-fluid rheology on the oil displacement process (Xia et al. 2001). Martel et al. conducted studies on the shear-thinning effect on oil displacement efficiency, and they posited that the shear-thinning behaviors of the injected polymer fluid could markedly raise the sweep efficiency (Martel et al. 1998).

In addition, there have been many studies aimed at evaluating the injectivity and resistance factors of the viscoelastic polymer solutions through experimental or theoretical methods. Mohammad tested the flow behavior of viscoelastic polymer solutions through various core-flooding experiments. He found a critical injection rate beyond which the polymer solutions manifest their viscoelastic effects, and the viscoelastic properties could be optimized according to the polymer molecular weights, polymer concentrations, and a variation in the degree of hydrolyzation (Ranjbar et al. 1992). Wang uncovered the rheological behaviors of polyacrylamide solutions through core experiments and found that the viscoelastic effect of polymers was exhibited under reservoir flow viscosity (Wang 1994). Wang found that the elastic properties of the polymer fluids could contribute to micro-scale recovery, and elastic effects should be considered when selecting the polymers for flooding (Wang et al. 2000). Zhang and Yue (2007) selected a numerical method to study the percolation mechanism of viscoelastic polymer solution through porous media. His study showed that the smaller throat sizes and greater viscoelasticity of the displacing fluid could lead to higher flow resistance. Xia et al. gave a detailed description of the elasticity of polyacrylamide fluid relative to the oil displacement efficiency. His study suggested that the contribution of the elasticity of the polymer solution to the oil displacement efficiency was approximately 40% (Xia et al. 2012).

When polymers are injected from the wellbore and are propagated into a deep reservoir, many factors can reduce the

effect of the performance, including high salinity, high temperatures and mechanical shearing. A great deal of work has been performed to modify the properties of polymers (Wu et al. 2012). Wu et al. conducted work on the synthesis of a linear-type post-hydrolyzed template copolymer for EOR synthesized with the following raw materials: acrylamide (AM), acrylic acid (AA), functional monomers such as the AMPS used for salt resistance and framework monomers. Compared to conventional HPAM, a linear polymer possesses stronger rigid chains, and thus an improved thickening behavior with high-temperature resistance and high-salinity tolerance (Wu et al. 2011). Taylor et al. studied the synthesis of HAHPAM, which contains a few hydrophobic groups on the side chains. Due to the hydrophobic effect, when a polymer dissolves in water, some of the hydrophobic groups may associate with one another, form super-molecular aggregations, and even a network structure, which induces a substantial increase in the solution viscosity (Taylor and Nasr-El-Din 1998). Therefore, to some extent, the HAHPAM can overcome the deficiencies of conventional polymers regarding high salinity and shear. Up until the present, HAHPAM has been one of the most commonly used polymers in the offshore oilfields in Bohai Bay (Zhou et al. 2006). Lei et al. researched the preparation of a newly modified polymer, the polymer–surfactant, and they found that the viscoelasticity could be improved substantially by forming a “surfactant micelle-like” structure (Lei et al. 2014).

Previous studies have mentioned the use of steady rheological measurements to obtain rheological characteristic curves of the specific polymers (Wever et al. 2011). Few have combined the steady rheological measurement with the radial flow in the field. Therefore, we aim at matching the shear rate in the rheological test with the radial flow velocity in the field to characterize the properties of the polymer solution, including the injectivity near the wellbore and the viscosity retention ability in deep reservoirs. In addition, many researchers have focused on the positive effects of elasticity in polymer solutions on oil displacement (Zhang et al. 2010), but few have analyzed the effects of elasticity on propagation behaviors. We, therefore, studied the propagation performance examined by both rheological methods performed in the testing containers, the sizes of which are much larger than the sizes of the molecular aggregations and the cyclotron radius of the polymer solutions (macroscopic dimension) and the sandpack flow of polymers in porous media for which the space size is far smaller or even the same order of magnitude as the polymer molecular sizes (microscopic dimension). We also analyzed the feasibility of using polymers for flooding during an entire process in terms of “injectivity to propagation” considerations. First, in accounting for the operational conditions of the offshore oilfields combined with the relatively high salinity of the target formation, common polymers can hardly satisfy the harsh

requirements. Therefore, these three newly modified polymers (linear polymer, HAHPAM, and polymer–surfactant) are suggested as potential candidates for polymer flooding in the Qikou oilfield. Second, rheological measurements, such as oscillatory, steady shear, and variable shear measurements, were performed to speculate about the propagation behavior of the tested polymers according to their rheological aspects. A sandpack flow experiment of viscoelastic polymer flooding was then constructed to evaluate the propagation properties of the three polymer solutions in porous media. Finally, the results for the propagation ability tested using rheological methods and the sandpack flow experiment are compared, and the corresponding microscopic mechanisms are examined in detail.

Results

Experiment

Experimental materials

Sandpack Figure 1 shows a schematic diagram of the sandpack flow experimental apparatus with the multi-point pressure taps used to determine the propagation performance of the three types of polymers. The sandpicks (ϕ 2.5 cm \times 50 cm) used in this article were all packed with sand (200 mesh) from Qikou in the Bohai Bay oilfield formation.

Chemicals The three polymers evaluated in this experiment are newly modified polymers. The linear polymer has a linear structure with an average relative molecular weight of 12 mDa. This polymer is manufactured by Shengju Refining and Chemical Company (Dongying, China). The linear polymer is technically mature during synthesis, and pilot tests have been performed in some oilfields, such as Daqing oilfield in China. One of its distinguishing characteristics is

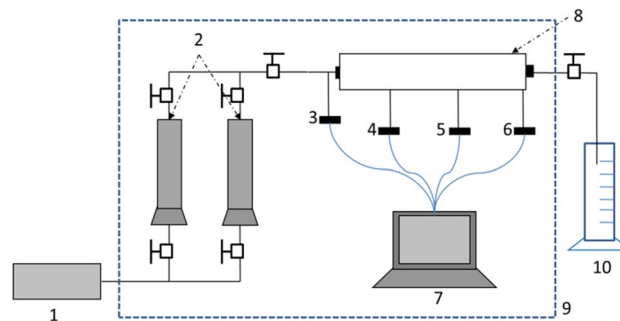


Fig. 1 Diagram of the sandpack flow process. 1—plunger pump; 2—container; 3— injection pressure tap; 4—pressure tap 1; 5—pressure tap 2; 6—pressure tap 3; 7—analysis computer; 8—sandpack; 9—oven; 10—measuring cylinder

its quick dissolution time in injected water. Usually, linear polymers at 2000 mg L^{-1} (the most widely used polymer concentration used for flooding) can be dissolved in water within 30 min, which is quite attractive for use in the polymer flooding process in oil fields, especially for offshore oilfields, due to limited surface facilities. HAHPAM was prepared via the copolymerization of acrylamide (AM) and sodium acrylate (NaAA) with *N*-(4-benzoyloxy)-acrylamide and dimethylaminoethyl methacrylate (DEAEMA), which contained a few hydrophobic groups on the side chains. Its viscosity-average molecular weight ($M\eta$) is 11 mDa. HAHPAM can overcome the deficiency found in conventional polymers regarding high salinity and shear. Up until now, HAHPAM has been one of the most commonly used polymers in offshore oilfields in the Suizhong oilfield of Bohai Bay. However, because of its type of aggregation structure, the dissolution of HAHPAM in injected water is much slower than that of the linear polymer, which may result in injectivity problems upon field application. The polymer was manufactured by Sichuan Guangya Refining and Chemical Company (Chengdu, China). The polymer–surfactant is also a type of newly modified polymer, and it is created by adding a functional monomer to the framework of the polymer molecule and forming a triaxial stereoscopic net structure, filling the entire system uniformly. Its average relative molecular weight is 7 mDa. The polymer was manufactured by Junlun Refining and Chemical Company (Shenzhen, China). The polymer–surfactant is a new type of modified polymer used for oil recovery, and it is created by adding a functional monomer to the framework of the polymer molecule and forming a triaxial stereoscopic net structure, filling the entire system uniformly, which shows characteristics of both polymers and surfactants and can improve the viscoelasticity substantially. It can be classified as a type of HPAM, and its average relative molecular weight is 7 mDa. The molecular structure of the polymer–surfactant is shown in Fig. 1.

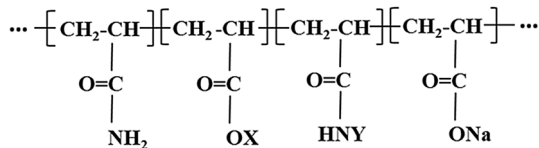


Fig. 2 Molecular structure of the polymer–surfactant (*X*, *Y* are functional groups by graft copolymerization)

Table 1 Composition of the simulated injection brines

Brine type	Cations			Anions				Total salinity
	Ca ²⁺	Mg ²⁺	Na ⁺	CO ₃ ²⁻	HCO ₃ ⁻	Cl ⁻	SO ₄ ²⁻	
Simulated injection brine (mg L ⁻¹)	568.9	228.9	2551.9	0	190.6	5470.7	36.6	9047.6

The polymer solution was prepared by adding the required amount of polyacrylamide to the simulated injection water. The polymer solutions were prepared in concentrations of 500, 600, 800, 1500, 2000, 3000, 4000, and 5000 mg L⁻¹ (Fig. 2).

Brine Brine water with a salinity of 9000 mg L⁻¹ was prepared so it would resemble the injection water from Block Qikou in the Bohai Bay Oilfield. The composition of the simulated injection brine is shown in Table 1.

Experimental procedure

Concentration dependence of three polymers The viscosity measurements of three types of polymer solutions were determined using an RS-6000 rheometer at the reservoir temperature (65 °C) at a constant shear rate. Given that the polymer fluid is a type of pseudoplastic solution, its viscosity changes with the applied shear rates, and thus only comparing the viscosities of polymer fluids under the same shear rate is rational. Because the shear rate applied to the injected polymer solutions under reservoir conditions is approximately 7.34 s^{-1} , the concentration dependence of HPAM and the long-term stability measurements were obtained at a shear rate of 7.34 s^{-1} (Melo et al. 2005).

Because a polymer's molecular conformations and aggregations could be affected by its concentrations, the polymer solutions were prepared by dissolving the three polymers in simulated injection water at various separate concentrations (500, 600, 800, 1500, 2000, 3000, 4000, and 5000 mg L⁻¹). We did not use simulated reservoir injection water to dilute the high-concentration polymer solution to obtain the low concentration one. In this study, all the tested polymer fluid samples were freshly prepared to minimize the degradation of the HPAM solution. When preparing the polymer solution of a required concentration, the accurately weighed polymer powder was added at a relatively slow speed to the simulated injection brine could be stirred at a high speed. After 5–10 min, the stirring speed was adjusted to a lower rate, and the prepared polymer fluid was stirred slowly for 24 h, to guarantee fully dissolved polymer solutions. After that, all the polymer solutions were stored in closed containers for further rheological and propagation behavior measurements.

Long-term thermal stability In the propagation test, the injected polymer fluids were kept under reservoir conditions for months. Many reservoirs of Bohai Bay oilfields show high

temperatures or even high-salinity properties, resulting in a certain degree of damage to the properties of the injected polymer solutions. Therefore, long-term high-temperature aging is highly necessary to investigate the polymer properties under unfriendly reservoir conditions.

Steady rheological behaviors of three polymers The apparent viscosity of various polymer solutions as a function of the shear rate ($\dot{\gamma}$) was measured using an RS-6000 rheometer (HAKKE) with a coaxial cylinder. The shear rate range was 0.1–100 s⁻¹; this range encompasses the shear rates of the injected fluid encountered near the wellbore and in the reservoir away from the wellbore (0.1–10 s⁻¹).

Oscillatory deformation tests of three polymers The viscoelastic properties of polymer solutions are widely used to gain insight into the structure and conformation of polymers in solution, and elastic modulus (G') also plays a key role in the propagation performance of polymers. Thus, oscillatory deformation tests of three polymer solutions were performed at 65 °C as well.

Oscillatory deformation tests on the freshly prepared polymer solutions were performed at a controlled shear rate mode with an RS-6000 Rheometer, using a Z40 DIN coaxial cylinder. The following two rheological measurement steps were performed:

- Deformation sweeps at a constant frequency (1 Hz) to determine the maximum deformation of the sample in the linear viscoelastic range.
- Frequency sweeps over a range of 0.1–100 Hz at an oscillating stress amplitude of 0.1 Pa. This value was within the linear viscoelastic region of the three polymer solutions, as determined by recording the amplitude sweeps at 1 Hz.

Constant shear rate of polymer solutions The flow of the polymer water solutions under shear was characterized at a reservoir temperature of 65 °C. Because most of the blocks in the Bohai Bay oilfields consist of sandstone formations formed by fluvial deposition with high porosity and low consolidation strength, the capillary bundle model of porous media could be used to determine the average pore radius. The calculation of the pore size can be evaluated using the following equation (Zaitoun and Kohler 1988):

$$r = (8k/\phi)^{1/2}. \quad (1)$$

Because Eq. (1) is appropriate for calculating the average pore radius under homogeneous unconsolidated media, we can obtain the shear rate of a given superficial velocity using Eq. (2) as put forward by Zitha et al. (1995):

$$\dot{\gamma} = \alpha \times 4vr, \quad (2)$$

where $v = q/A\phi$ is the superficial velocity and α is a parameter that was found to be equal to 2.5 for particles with angular shapes.

According to Eq. (2), a superficial velocity of 0.5 mL min⁻¹ corresponds to a shear rate of 104.4 s⁻¹ during the constant shear rate measurement.

Propagation performance A brief summary of the experimental procedure for this section is as follows:

1. The sandpicks used for the polymer flooding process were packed with sand at a 200 mesh size that was saturated with simulated injection brine.
2. Permeability measurement by water was conducted by injecting the simulated injection water at a rate of 2 mL min⁻¹ until a constant pressure drop was achieved. The permeability was calculated according to Darcy's equation.
3. Several pore volumes of polymer solution were then injected into the sandpick at a flow rate of 0.5 mL min⁻¹. The multi-point pressure was measured at different aging times. According to the pressure changes, it can be inferred whether the polymer solution can achieve good propagation performance or not in porous media.

Materials and methods

Concentration dependence of HPAM

The variation in viscosity as a function of the polymer concentration at 65 °C is plotted in Fig. 3. The changes in the rising speed of the viscosity with the concentrations are more

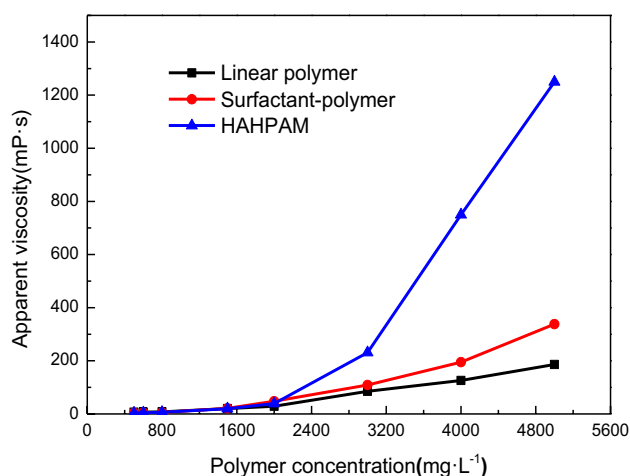


Fig. 3 Apparent viscosity plotted as a function of concentration for HAHPAM, surfactant-polymer, and linear polymer in brine (salinity = 9000 mg L⁻¹, [Ca²⁺] + [Mg²⁺] = 900 mg L⁻¹, $T = 65$ °C, concentrations vary from 0.05 to 0.5 wt%, $\dot{\gamma} = 7.34$ s⁻¹)

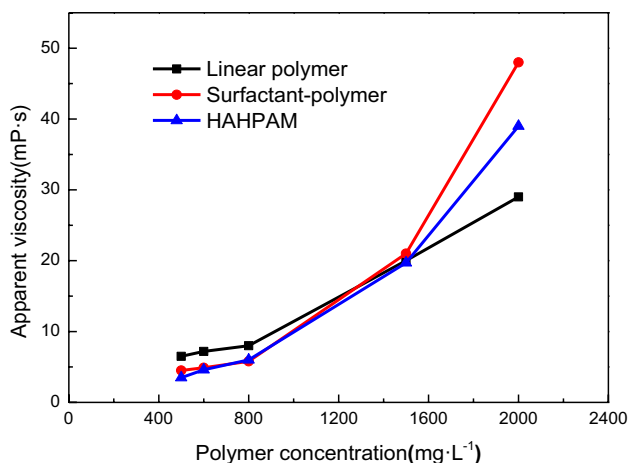


Fig. 4 Apparent viscosity plotted as a function of concentrations for HAHPAM, surfactant–polymer, and linear polymer in brine (salinity = 9000 mg L⁻¹, [Ca²⁺] + [Mg²⁺] = 900 mg L⁻¹, T = 65 °C, concentrations vary from 0.05 to 0.2 wt%, $\dot{\gamma} = 7.34 \text{ s}^{-1}$)

clearly established in Fig. 4, in which the rising trend in viscosity becomes more distinct when the concentration reaches approximately 0.08 wt%.

Below this concentration, the van der Waals' forces and hydrogen bonds are not strong enough to form a three-dimensional space network structure with relatively small hydrodynamic volumes. Therefore, the rising trend in the viscosity of HAHPAM and polymer–surfactant with concentrations from 500 to 800 mg L⁻¹ is lower than that of the linear polymer (Fig. 3). Above 0.08 wt%, the viscosities of HAHPAM and polymer–surfactant increased dramatically. This finding suggests that 0.08 wt% is the critical association concentration (CAC) of the HAHPAM and polymer–surfactant, above which the polymer–surfactant molecules interact with one another through nodes and chains and form a super-molecular structure, which is some type of “dynamic crosslinking network structure” that significantly increases the viscosity of the polymer solution. Intermolecular hydrophobic associations play a key role in the solution above the CAC.

The permeability of the Qikou oilfield is primarily in the range of 500–1000 mD. The formation type is sandstone, and the average porosity is approximately 0.31. According to Eq. (1), the average radius is 3.6–5.1 μm . According to Eq. (2), a shear rate of 7.34 s⁻¹ is equal to a flow rate of 2.64 $\times 10^{-6}$ to 3.73 $\times 10^{-6}$ m s⁻¹. The average water/polymer injection rate Q is 500 m³ day⁻¹. The shear rate of 7.34 s⁻¹ then corresponds to the distance from the wellbore that can be calculated as follows:

$$v = \frac{Q}{2\pi RH\phi}, \quad (3)$$

where v is the flow velocity, Q is the water/polymer solution injection rate, R is the distance from the wellbore, H is

the thickness of the injection layer, and ϕ is the formation porosity.

From Eq. (3), we can find that a shear rate of 7.34 s⁻¹ corresponds to the velocity at 80–112 m from the wellbore. The distance between the injection well and the production well in Qikou oilfield is 200–500 m. Therefore, a shear rate of 7.34 s⁻¹ represents the velocity in the deep reservoir.

Long-term stability measurements

Figure 5 shows the variation in the viscosity as a function of the aging time for the HAHPAM, polymer–surfactant, and linear polymer solutions with aging at 65 °C and a 0.2 wt% concentration.

The results indicate that the changing trend in polymers with hydrophobic association groups (polymer–surfactant and HAMHPAM) differs from that of the linear polymer.

When the linear polymer is prepared, the solution is in a balanced and homogeneous state. The viscosity of the “0.2% linear polymer” is 29 mPa s, and it drops down to 15.6 mPa s after 7 days, with a viscosity loss of 46.21%. By contrast, one can clearly observe a sharp increase in the viscosity for HAHPAM and polymer–surfactant after continuous aging for 3 days; the initial viscosities (0 day) of HAHPAM and polymer–surfactant are 39 and 48 mPa s, respectively, but they increase to 188 and 87 mPa s, respectively, after 3 days of aging, for 510 and 181% increases in the viscosity. After 7 days, the reduction in the viscosities of the HAHPAM and polymer–surfactant is not serious. The reasons for the decline in the viscosity of the three polymers are due to oxygen, bacteria, and other external conditions. In addition, another important factor causing the decline of polymer viscosity in Fig. 5 is assumed to be spontaneous over-hydrolysis. These results clearly demonstrate that HAHPAM and

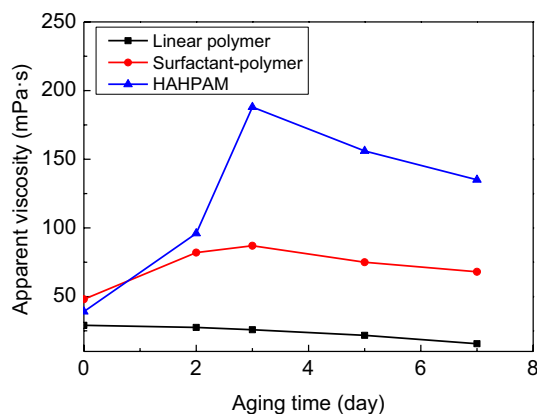


Fig. 5 Long-term thermal stability of 0.2 wt% linear polymer, 0.2 wt% surfactant–polymer, and 0.2% HAHPAM polymer (salinity = 9000 mg L, [Ca²⁺] + [Mg²⁺] = 900 mg L⁻¹, $\dot{\gamma} = 7.34 \text{ s}^{-1}$). Both the aging and measuring temperatures are 65 °C

polymer–surfactant solution possess much better long-term thermal stability than the linear polymer. This difference is primarily ascribed to the relatively long process of building a homogeneous three-dimensional network of HAHPAM and polymer–surfactant solution. When interaction forces remain balanced, the solution reaches the maximum value. The results also indicate that there are balanced binding forces caused by hydrophobic associations, hydrogen bonding, and van der Waals' force to prevent the hydrolysis of amide groups that occur under reservoir conditions.

Steady rheological behaviors of three polymers

In relation to a field injection of the polymer solution in a specific polymer flooding process, the fluid velocities are the highest in the vicinity of injection or production wellbores, but they rapidly decline as the distance from the wellbore increases. The displacing-fluid injection rates vary, depending on the effective mobility of the displacing fluid at a given stage of the flood.

Our central objective is to combine the steady rheological measurement with the radial flow in the field. In other words, we would like to match the shear rate in the rheological test with the radial flow velocity in the field. This approach is relatively novel. For a better characterization of the radial flow in the field, we used logarithmic coordinates for shear rates. The viscosity measured at high shear rates reflects the viscosity near the wellbore or around the injection area, while the viscosity tested at low shear rates indicates the viscosity in the deep reservoir. The flow of three polymer solutions under shear is characterized at the reservoir temperature of 65 °C. Figure 6 shows the experimental results for the viscosity (mPa s) versus the shear rate (s^{-1}) for 2000 $mg L^{-1}$ solutions to cover the effects of the low, medium, and high shear rates on the polymer viscosities. Based on the results from Fig. 6, we could conduct a preliminary screening on the suitable polymer according to the criteria of low viscosity (good injectivity) near the wellbore and high viscosity (good viscosity retention ability) in the reservoir.

The results show that the viscosity of the linear polymers decreases with the increased shear rates, exhibiting pseudoplastic behavior. However, there was an initial increase in the viscosity of the HAHPAM and polymer–surfactant with the rising shear rates ($\dot{\gamma} < 0.2 s^{-1}$). Most of the conventional polymer fluids are known to show Newtonian behavior at low shear rates, exactly like the linear polymer performs at low shear rates in Fig. 6. Because the structural morphology caused by either hydrophobic grouping or surfactant micelle-like aggregations exists in the two polymers (HAHPAM and polymer–surfactant) at low shear rates, the forces driving the molecular chains oriented towards the shearing direction (shear thinning) are smaller than the forces directing the molecular aggregations that are getting close to each

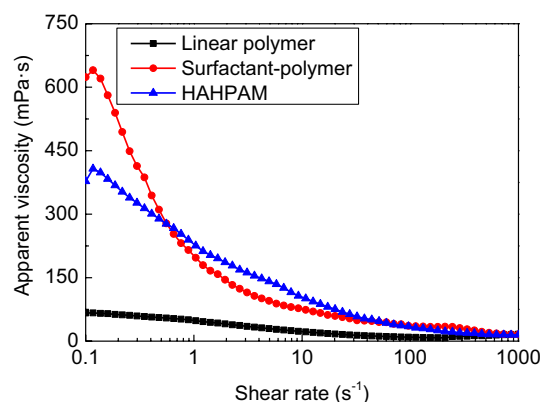


Fig. 6 Apparent viscosity plotted as a function of 0.2 wt% linear polymer, 0.2 wt% surfactant–polymer, and 0.2% HAHPAM polymer, $C_p=0.2$ wt%. (salinity=9000 $mg L^{-1}$, $[Ca^{2+}] + [Mg^{2+}] = 900$ $mg L^{-1}$, $\dot{\gamma}$ ranges from 0.1 to 1000 s^{-1}). Both the aging and measuring temperatures are 65 °C

other to form a temporary larger structure (similar to the shear thickening phenomenon of suspending liquid). Therefore, at low shear rates, the initial rise in the viscosity of the two polymers (HAHPAM and polymer–surfactant) occurred. With the increase in the shear rates, the former factor is coming to play a key role, indicating a shear-thinning effect. We suspect that the high shear thinning of the polymer–surfactant and HAHPAM is a consequence of the uncoiling and aligning of the polymer chains along the flow direction.

Typical viscosity–shear rate data for the three polymers are presented in the curves. The three polymer solutions exhibited non-Newtonian flow and shear-thinning behavior, as expected. The commonly used flow models, such as Bingham, Casson or Carreau, can be applied to characterize the flow behaviors of the HPAM solutions. Compared to other flow equations, the Carreau model (Eq. 4) is more suitable for providing a satisfactory description of the flow behavior of the above three polymer solutions, as follows:

$$\eta = \eta_0(1 + (\lambda\dot{\gamma})^2)^{\frac{n-1}{2}} \quad 0 < n < 1, \quad (4)$$

where η is the apparent viscosity (mPa s), K is the consistency coefficient (Pa s), $\dot{\gamma}$ is the shear rate (Pa), and n is the flow behavior index (dimensionless), a material parameter that determines the shear-thinning nature.

The rheological parameters for the three polymer solutions are shown in Table 2 for the Carreau model related to Eq. 3. All the samples exhibited a good fit to the Carreau equation. Because the flow behavior indexes (n) were below 1 for the three tested polymer solutions, the three polymers can all be classified as pseudoplastic fluids. It is worth noting that the shear-thinning behavior of the linear polymer was less remarkable than that of the other two polymers. As shown in Table 2, the flow behavior index n indicates more

Table 2 Carreau model data analysis for three polymer solutions (2000 mg L⁻¹)

Polymer type	η_0	λ	n	R^2
Linear	66.4364	-2.9289	0.6987	0.9736
Polymer-surfactant	910.0524	-14.9957	0.4771	0.9913
HAHPAM	407.5443	4.4959	0.6264	0.9959

significant shear-thinning behavior for the polymer-surfactant and for HAHPAM.

According to Table 2, the power-law equations of the polymer-surfactant and HAHPAM achieved satisfactory fits, indicating good pseudoplastic behavior; the consistency coefficient of polymer-surfactant and hydrophobic associations are relatively large, indicating a more viscous fluid; and the n values of the polymer-surfactant and HAHPAM are small, indicating severe shear-thinning behavior.

From Fig. 6, we can also observe that when polymer solutions are being injected into the reservoir, polymer solutions are under high shear rates and the viscosity of all three polymer solutions are low, indicating good injectivity. Considering the production rate of the Qikou oilfield and the moving rate of displacement fluid in the reservoir, which was approximately 0.2–0.5 m day⁻¹, the shear rates are thus in the range of 5.88–14.42 s⁻¹. From Fig. 6, we can observe that the viscosity of the HAHPAM is the highest within this range, indicating a good oil-displacing capability. That finding is followed by the polymer-surfactant, whereas the linear polymer maintains the lowest viscosity at low shear rates.

For example, the viscosity of “0.2% HAHPAM” at 7.34 s⁻¹ is nearly five times larger than that of the 0.2% linear polymer solution at 65 °C. Additionally, from the steady rheological test, all three polymer solutions obtain good injectivity and propagation properties, and the HAHPAM and polymer-surfactant solutions show better viscosity retention away from the wellbore and in the deep reservoir.

Oscillatory deformation tests

In this section, analyses on the dynamic rheological behaviors for the tested samples were performed. Two important rheological parameters, the elastic modulus (G') and the viscous modulus, were used to reflect the viscoelasticity of the three polymers. G' is a measure for the energy stored reversibly in the system. G'' reflected the energy that was dissipated because of deformation.

Deformation sweep result

To guarantee all the tested samples in the linear viscoelastic range, appropriate shear rates should be applied to keep constant values for G' and G'' . Changes in the G' and G''

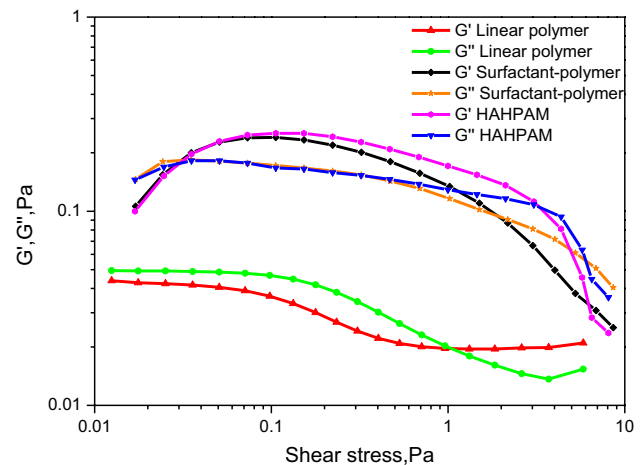


Fig. 7 Storage modulus (G'), and viscous modulus (G''), plotted as a function of shear stress for HAHPAM, linear polymer, and surfactant-polymer in brine (salinity=9000 mg L⁻¹, [Ca²⁺] + [Mg²⁺] = 900 mg L⁻¹, $T = 65$ °C, concentrations = 0.2 wt%)

values of the three polymer solutions ($C_p = 2000$ mg L⁻¹) are shown in Fig. 6.

From Fig. 7, we can observe that the linear viscoelastic range is within 0.01–0.1 Pa. For the polymer-surfactant and HAHPAM solutions, when the shear stress was smaller than the critical shear rate (0.15 Pa), the G' was much greater than the G'' , indicating that an elastic nature prevailed over a viscous nature. For the linear polymer solution, the G'' was larger than the G' , showing a more viscous behavior. However, one can notice that when the shear stress is larger than the critical shear rate, there is a decreasing trend for both the G' and the G'' . The decreasing phenomena of the two viscoelastic parameters are connected to the changing molecular conformations, which result from the helix-coil transition of the polymer solutions. Moreover, we surprisingly notice that the linear viscoelastic region for the HAHPAM and polymer-surfactant is wider than that of the linear polymer solution. We suspect the reason for this phenomenon is that when the stress amplitude exceeds the linear viscoelastic range, the chains of the linear polymer gradually extend with the increase in shear stress, showing non-linear extension. For the HAHPAM and polymer-surfactant, their extension abilities are weaker than that of the linear polymer. When external shear stresses are applied to the HAHPAM and polymer-surfactant solutions, the two polymers only show limited deformation to store energy. With the increase in the external forces, structural changes will not occur due to the deformation of the HAHPAM and polymer-surfactant, and only subtle deformations of parts of the polymer chains may occur. Therefore, the linear viscoelastic region for the HAHPAM and polymer-surfactant is wider than that of the linear polymer solution. Moreover, HHPAM and polymer-surfactant solutions are more sensitive to shear stress when the

shear stress is greater than the critical shear rate. The linear polymer stretches with the increase in shear stress, indicating a non-linear extensibility. Due to the strong association forces in the HAHPAM and polymer–surfactant, their extensibility abilities are much weaker.

Frequency sweep result

Figure 8 presents the frequency sweeps for three polymer solutions at 65 °C ($C_p=2000 \text{ mg L}^{-1}$). As observed from the plots, for the HAHPAM and the polymer–surfactant, the G' was much greater than the G'' at all the frequency values, showing that for a predominant elastic behavior, the G' increased with the increase in frequencies, whereas the G'' was less dependent on the frequency.

Moreover, a crossover between these two moduli (G' and G'') in the HAHPAM and polymer–surfactant was not found during the entire frequency sweep test (with frequencies ranging from 1 to 100 Hz). The relatively high values of the G' reflected in the above test could be partly related to the rigid conformation of the polymers in these two solutions, reflecting the much lower flexibility of the polymer chains in the two solutions (HAHPAM and polymer–surfactant) than that of the linear polymer, which reflected a random coil conformation. Therefore, the rigid conformation and distinct elastic properties of the HAHPAM and polymer–surfactant brought about a much stronger three-dimensional network in the two polymer solutions.

In addition, the fluctuation of the linear polymer is less severe than that of the polymer–surfactant and HAHPAM. The reason for the fluctuations in the polymer–surfactant and HAHPAM is as follows. Due to crosslinking forces between the molecular chains combined with the aggregation forces

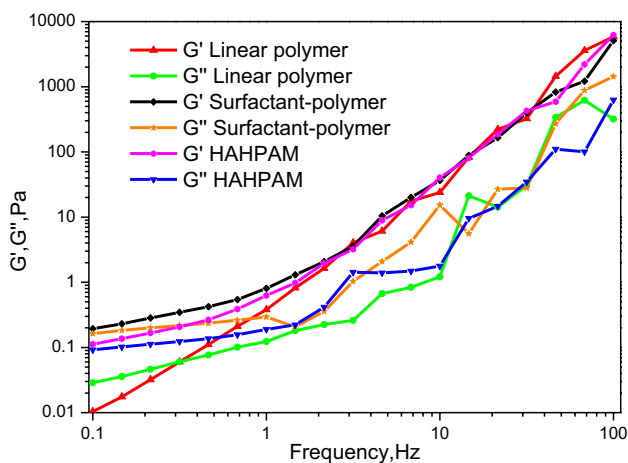


Fig. 8 Storage modulus, (G') and viscous modulus, (G'') plotted as a function of frequency for HAHPAM, linear polymer, and surfactant–polymer in brine (salinity=9000 mg L^{-1} , $[\text{Ca}^{2+}] + [\text{Mg}^{2+}] = 900 \text{ mg L}^{-1}$, $T = 65 \text{ }^\circ\text{C}$, concentrations=0.2 wt%)

of hydrophobic groupings for the polymer–surfactant and HAHPAM, the two polymer solutions form a “regional” three-dimensional structure of polymer molecular aggregations, showing more heterogeneous characteristics than the linear polymer solution. Therefore, the frequency sweep results of the HAHPAM and polymer–surfactant present more fluctuations than the linear polymer solution. In addition, we conducted TEM analyses of the three polymer solutions to study the internal structure. From the TEM results, we can see that the three polymers present different molecular structures. The linear polymer shows the long-chain structure and the electrostatic repulsion between intermolecular chains is strong, and thus the molecular chain conformation is stretching. For the HAHPAM solution, the molecular chains of the polymers can cross one another, forming a random network structure. For the polymer–surfactant solution, there are coarse trunks and fine branches in the solution, and it appears to be a “slice-network” structure because the molecular chain combines short side chains with polar groups, and the active groups are grafted. Therefore, the extension ability of the primary chain is improved (Fig. 9).

Constant shear rate test

When all three polymer solutions ($C_p = 2000 \text{ mg L}^{-1}$) are under a constant shear rate of 104.4 s^{-1} for 300 s, the fluctuations in viscosity are more distinct for the HAHPAM and polymer–surfactant solutions than for the linear polymer solutions. For the HAHPAM solution, the fluctuation in viscosities is 28.75%; for the polymer–surfactant solution, the variation is 18.99%. The linear polymer shows an almost constant value with 4.96% in fluctuations. Under a constant shear rate of 104.4 s^{-1} , the polymer–surfactant shows the largest viscosity value of 19.00 mPa s, then a polymer–surfactant value of 14.71 mPa s. The linear polymer shows the lowest polymer viscosity of 7.67 mPa s (Fig. 10).

Propagation performance

Three sandpack flow experiments were performed to investigate and compare the propagation of three polymer solutions ($C_p = 2000 \text{ mg L}^{-1}$) under a simulated Qikou Formation in the Bohai Oilfield reservoir environment. In this case, the injection rate we use is 0.5 ml min^{-1} . Because the injection rate for the Qikou oilfield is $500 \text{ m}^3 \text{ day}^{-1}$ and we want to study the propagation behavior of the polymer solution, we simulated the behavior of the polymer solutions flowing from the wellbore to the deep reservoir, at approximately 5–7 m from the wellbore. From $v = q/(2\pi Rh)$, we can calculate v , where R is the distance from the wellbore and h is the depth of the pay zone. Injection rate Q for the core-flooding test can then be calculated from the following equation: $Q = \pi r^2 v = 0.5 \text{ mL min}^{-1}$.

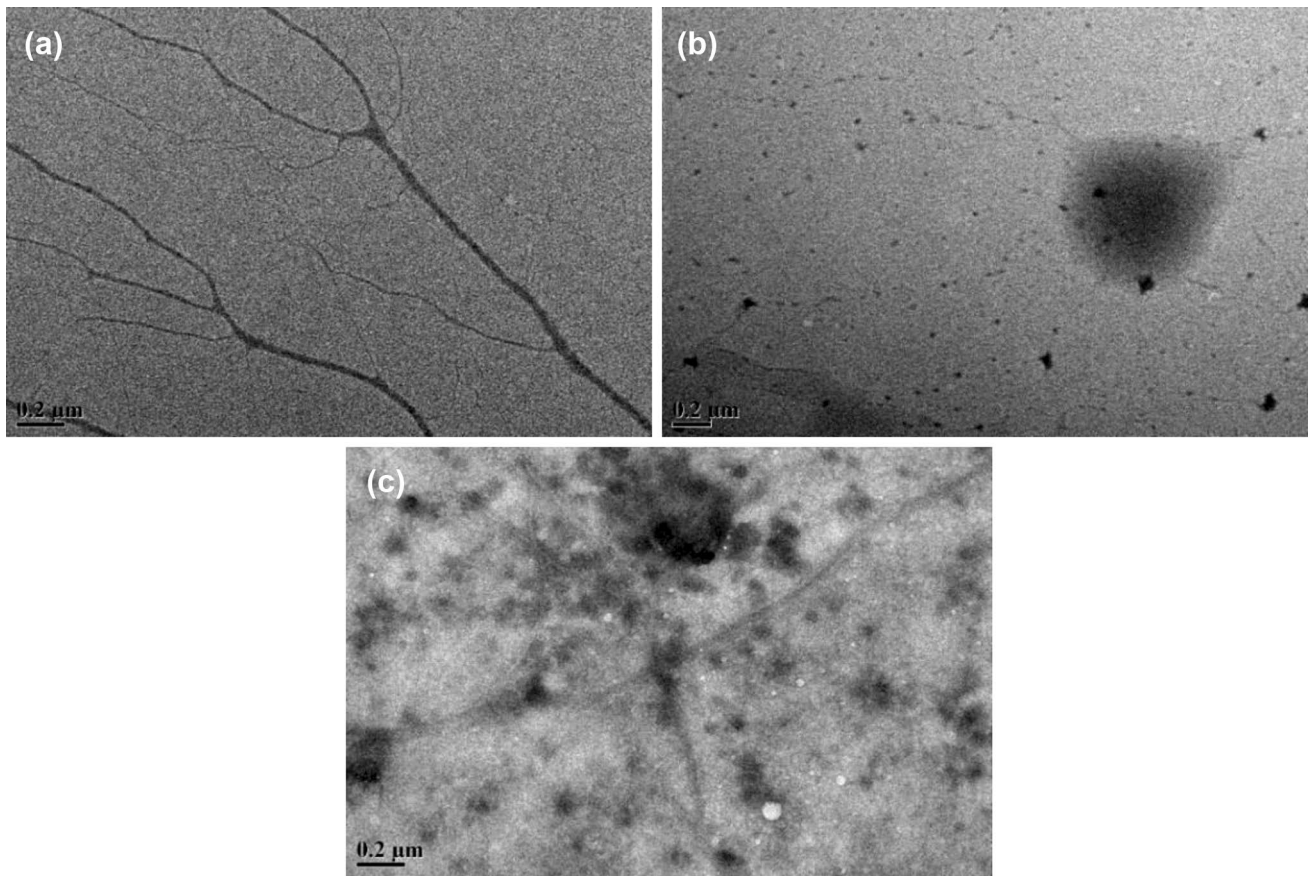


Fig. 9 a TEM image of linear polymer; b TEM image of polymer–surfactant; and c TEM image of HAHPAM

The pressure profiles of the three testing points for the three polymer solutions during the injection period are shown in Fig. 11. The pressure profiles of the linear polymer and the polymer–surfactant are similar, but the pressure

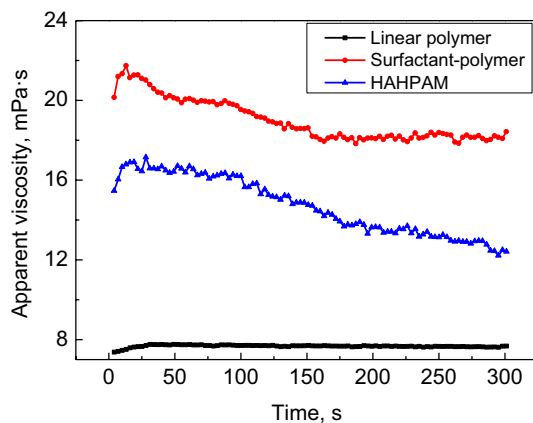


Fig. 10 Viscosity plotted as a function of time for HAHPAM at a constant shear rate of 104.40 s^{-1} , linear polymer, and surfactant–polymer in brine (salinity = 9000 mg L^{-1} , $[\text{Ca}^{2+}] + [\text{Mg}^{2+}] = 900 \text{ mg L}^{-1}$, $T = 65 \text{ }^\circ\text{C}$, $C_p = 0.2 \text{ wt\%}$)

build-up during the HAHPAM solution injection is much faster than it is for the other two polymer solutions. The pressure gradients of the three polymer solutions are summarized in Fig. 12. Not surprisingly, the linear polymer solution can be transported into the deep area of the sandpack constantly, due to its linear polymer structure.

In addition, we find that the elastic polymer–surfactant shows the best propagation behaviors. The polymer–surfactant can be injected easily and transported smoothly within the sandpack. In addition, the injection pressure is relatively small during the entire injection process and the resistance (pressure) can be tested for all three pressure taps. We speculate that although the average size of the molecular aggregations for the polymer–surfactant solution is 500–600 nm (Lu et al. 2016) depending on the deformation properties of the polymer–surfactant solution, the aggregations can still propagate well in the sandpack, and they can maintain a relatively high pressure in the deep sandpack.

For HAHPAM solutions, the elastic polymer solutions cannot be injected into the sandpack smoothly, and many elastic polymer solutions gather at the injection end of the sandpack and in the injection pipeline. The injection pressure then increases rapidly as shown in Figs. 11 and 12. Only

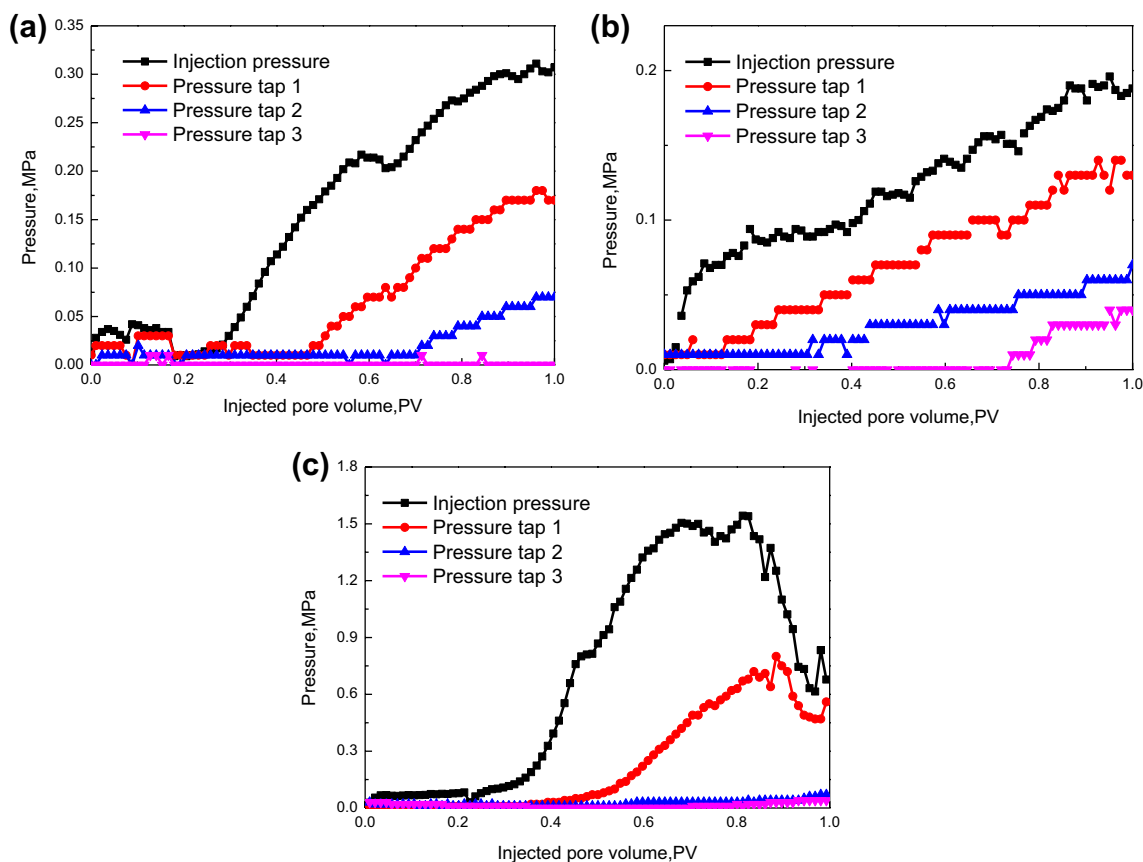


Fig. 11 Injection pressure, pressure of tap 1, pressure of tap 2, and pressure of tap 3 plotted as a function of injected volume of samples: **a** 0.2% linear polymer, **b** 0.2% surfactant–polymer, and **c**

0.2% HAHPAM (permeability=600 mDa, salinity=9000 mg L⁻¹, [Ca²⁺]+[Mg²⁺]=9000 mg L⁻¹, T=65 °C, concentrations=0.2 wt%, injected volume=1 PV, injected rate=0.5 mL min⁻¹)

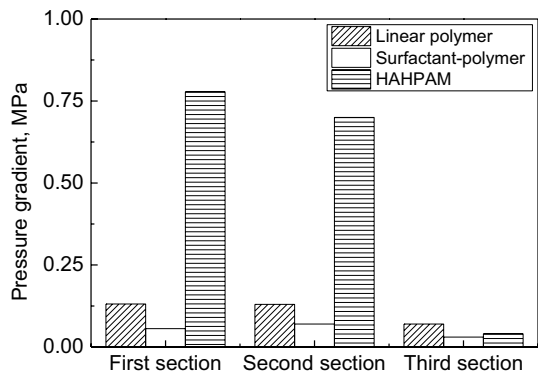


Fig. 12 Maximum pressure gradients of three sections for linear polymer, surfactant–polymer, and HAHPAM (permeability=600 mD, salinity=9000 mg L⁻¹, [Ca²⁺]+[Mg²⁺]=9000 mg L⁻¹, T=65 °C, concentrations=0.2 wt%, injected volume=1 PV, injected rate=0.5 mL min⁻¹)

a small section of HAHPAM solutions can be injected into the sandpack. Thus, the pressures tested in three pressure taps are very low. The reason for the bad propagation behavior of HAHPAM is as follows. Due to crosslinking forces

between its molecular chains combined with the aggregation forces of its hydrophobic groupings, the “regional” three-dimensional structure of polymer molecular aggregations are formed for HAHPAM solutions, which show high viscosity and elastic properties in macroscopic dimensions. According to conventional opinion, good elasticity is helpful for the oil recovery process. In fact, the molecular configuration of HAHPAM shows more advantages than the linear polymer for obtaining a greater viscosity and elasticity. However, the “real work environment” for the polymer solution is the reservoir porous media, the space size of which is far smaller than that of the container used for preparing the polymer solution indoors. Therefore, the HAHPAM solution that contains large molecular aggregations may have adaptability problems with oil reservoirs. According to Figs. 11 and 12, although the injection pressure of HAHPAM is large, at the central and deep parts of the sandpack, the pressure gradient is relatively low (from pressure tap 2 to tap 3). We can thus conclude that the HAHPAM cannot flow into the deep part of the sandpack. The primary changes in the pressure gradients of the HAHPMA solution are in and near the injection

Table 3 Summary of polymer molecular sizes and propagation behavior in the sandpack

Polymer type	Molecular cyclotron radius, r_p (μm)	Pore throat radius, r_h (μm)	r_h/r_p	Propagation result
Linear polymer	0.28	4.00	14.29	Good
Surfactant–polymer	0.52	4.00	7.69	Good
HAHPAM	1.22	4.00	3.28	Bad

area of the sandpack, and the HAHPAM failed to establish an effective displacing pressure gradient inside the sandpack.

The results showed the great differences in the injectivity and propagation properties between the rheological tests and the sandpack tests. We speculate that the differences resulting from the microscopic behaviors are not similar to the performance evaluations under macroscopic conditions, especially for polymers with spatial networks. The test conducted in the steady and core rheological behavior measurements pertain to the macroscopic dimension. The sandpack test relates to the microscopic dimension. Under porous media conditions, the chains of the high molecular polymer can cross or wind with one another, bringing about the building of a structure of a strong and intense three-dimensional network in the solution. The polymer molecular weight of the HAHPAM is greater than that of the polymer–surfactant. The larger the molecular weight, the longer the molecular chain of the polymer (Zhao et al. 2011; Huang et al. 2017). In addition, the intermolecular force is enhanced by the larger molecular space network structure, resulting in the molecular cyclotron radius of the HAHPAM being the largest, and thus it has the worst propagation ability in the sandpack under microscopic conditions.

To support the above speculation more, we measured the molecular aggregation sizes of the HAHPAM and polymer–surfactant, and the molecular cyclotron radius (r_p) of the linear polymer. In this test, the r_p is obtained by DLS method with a Malvern Zetasizer nano-range device. The sizes of the pores in the sandpack (r_h) are calculated from Eq. (1). The data are shown in Table 3, concerning the Qikou reservoir. The ratios of the pore throats to the polymer molecular cyclotron radiuses or polymer molecular aggregation sizes in the linear polymer and polymer–surfactant are greater than the ratios in the HAHPAM system. The polymer molecular sizes and propagation behavior in the sandpack are summarized in Table 3.

In the microscopic dimension, the flow of a given polymer could be affected by many variables. In addition to the molecular conformation discussed in the rheological tests, the compatibility of the macromolecular dimension to the pore throat size (the ratio between the pore throat radiuses to the polymer molecular cyclotron radius) and the retention

of polymer viscosity during propagation have a great impact on the transport of polymer solutions in the porous media.

Conclusions

- The three polymers selected for this study are based on requirements for time-saving dissolution and good salt resistance. Additionally, steady-state rheological measurements were performed to match the shear rate in the rheological test with the radial flow velocity in the field behaviors. Based on these results, we conducted a preliminary screening on the suitable polymer according to the required criteria of low viscosity (good injectivity) near the wellbore and high viscosity (good viscosity retention ability) in the reservoir. All three polymer solutions showed good injectivity, and the HAHPAM and polymer–surfactant solutions showed better viscosity retention away from the wellbore and in the deep reservoir.
- Propagation performance: the pressure build-up during HAHPAM solution injection is much faster than that of the linear polymer and polymer–surfactant. The results showed the substantial differences in the injectivity and propagation properties between the rheological analysis and the sandpack tests. The compatibility of the macromolecular dimension for the given pore throat sizes and the retention of polymer viscosity have a great impact on the transport of polymer solutions in the porous media.
- The results obtained from the sandpack flow experiments contrasting with the rheological measurements indicated that good viscoelastic performance within the rheological behaviors is not equivalent to good propagation behavior in porous media. The selectivity of polymers for flooding should be analyzed by considering the whole process. Reservoir adaptability should be considered in combination with rheological behaviors when selecting polymers for chemical flooding. Based on the results, we recommend the polymer–surfactant as the most suitable choice for polymer flooding in the Qikou oilfield. Although its apparent viscosity is relatively low, the linear polymer could be another candidate due to its acceptable propagation behaviors and favorable surface facility investments.

Acknowledgements The authors wish to express their appreciation for the funding provided by the National Science and Technology Major Project of China (2016ZX05058), the Science and Technology Foundation for Selected Overseas Chinese Scholar of Tianjin, and the Important Science and Technology Foundation of China Oilfield Service Limited (YSB16YF001).

Author contributions LT and MY contributed to all parts of the process of this study, developing the theoretical methodology, designing the

experimental procedures, conducting the experiments, and writing the paper; and XL, BZ, and YZ analyzed the data. WL revised the paper.

Compliance with ethical standards

Conflict of interest The authors declare no conflict of interest.

Open Access This article is distributed under the terms of the Creative Commons Attribution 4.0 International License (<http://creativecommons.org/licenses/by/4.0/>), which permits unrestricted use, distribution, and reproduction in any medium, provided you give appropriate credit to the original author(s) and the source, provide a link to the Creative Commons license, and indicate if changes were made.

References

- Acharya A (1986) Particle transport in viscous and viscoelastic fracturing fluid. *SPE Prod Eng* 1:104–110
- Alvarado V, Manrique E (2010) Enhanced oil recovery: an update review. *Energies* 3(9):1529–1575
- Chang HL, Zhang ZQ, Wang QM, Xu QM, Guo ZD, Sun HQ, Cao XL, Qiao Q (2006) Advances in polymer flooding and alkaline/surfactant/polymer processes as developed and applied in the People's Republic of China. *J Pet Technol* 58:84–89
- Cheng JC, Wang DM, Wu JZ (2000) Molecular weight optimization for polymer flooding. *Acta Pet Sin* 21:102–106
- Delamaide E (2014) Polymer flooding of heavy oil—from screening to full-field extension. In: Paper SPE 171105 presented at the SPE heavy and extra heavy oil conference: Latin America, 24–26 Sept, Medellín, Colombia
- Huang B, Zhang W, Xu R (2017) A study on the matching relationship of polymer molecular weight and reservoir permeability in ASP flooding for Duanxi reservoirs in Daqing oil field. *Energies* 7:951–962
- Lei QL, Ge HJ, Yang WH, Cheng J, Liu N (2014) Preparation method of one polymer-surfactant for oil-displacement: China. CN 104231165A
- Lu X, Hu G, Cao W (2016) Influences of the polymer retention characteristics on the Enhanced Oil Recovery of the chemical flooding. *Petrol Geol Oilfield Dev Daqing* 3:99–105
- Martel KE, Martel R, Lefebvre R, Gelin PJ (1998) Laboratory study of polymer solutions used for mobility control during in situ NAPL recovery. *Ground Water Monit Remediat* 18:103–113
- Melo MA, Holleben CR, Silva IG (2005) Evaluation of polymer-injection projects in Brazil. In: SPE Latin American and Caribbean petroleum engineering conference, Rio de Janeiro, Brazil, 20–23 Jun 2005
- Ranjbar M, Rupp J, Pusch G, Meyn R (1992) Qualification and optimization of viscoelastic effects of polymer solutions for enhanced oil recovery. In: Proceedings of the SPE/DOE eighth symposium on EOR, Tulsa, Oklahoma, USA, 22–24 April 1992
- Saboorian-Jooybari H, Dejam M, Chen Z (2015) Half-century of heavy oil polymer flooding from laboratory core floods to pilot tests and field applications. In: Paper SPE 174402 presented at the SPE Canada heavy oil technical conference, Calgary, Alberta, Canada, 9–11 Jun
- Saboorian-Jooybari H, Dejam M, Chen Z (2016) Heavy oil polymer flooding from laboratory core floods to pilot tests and field applications: half-century studies. *J Pet Sci Eng* 142:85–100
- Seright RS (2016) How much polymer should be injected during a polymer flood? In: Paper SPE 179543 presented at the SPE improved oil recovery conference, 11–13 April, Tulsa, Oklahoma, USA
- Silva IG, de Melo MA, Luvizotto JM, Lucas EF, Polymer Flooding (2007) A sustainable enhanced oil recovery in the current scenario. In: Proceedings of Latin American and Caribbean petroleum engineering conference, Buenos Aires, Argentina, 15–18 Apr 2007
- Smith F (1970) Behavior of partially hydrolyzed polyacrylamide solutions in porous media. *J Pet Technol* 22:148–156
- Sofia GB, Djamel A (2016) A rheological study of Xanthan polymer for enhanced oil recovery. *J Macromol Sci Part B* 55:204–206
- Standnes DC, Skjevraak I (2014) Literature review of implemented polymer field projects. *J Pet Sci Eng* 122:761–775
- Taylor KC, Nasr-El-Din HA (1998) Water-soluble hydrophobically associating polymers for improved oil recovery: a literature review. *J Pet Sci Eng* 19:265–280
- Wang W (1994) Viscoelasticity and rheological property of polymer solution in porous media. *J Jiangnan Pet Inst* 16:54–57
- Wang D, Cheng J, Yang Q (2000) Viscous-elastic polymer can increase microscale displacement efficiency in cores. In: SPE annual technical conference and exhibition, Dallas, Texas, USA, 1–4 Oct 2000
- Wever DAZ, Picchioni F, Broekhuis AA (2011) Polymers for enhanced oil recovery: a paradigm for structure-property relationship in aqueous solution. *Prog Polym Sci* 36:1558–1628
- Wu FP, Zhang YL, Zhang YX, Shi MQ (2011) Preparation method of one salt and heat resistance HPAM: China. CN 102060965A
- Wu YE, Mahmoudkhani A, Watson P (2012) Development of new polymers with better performance under conditions of high temperature and high salinity. In: Proceedings of the SPE EOR conference at oil and gas West Asia, Muscat, Oman, 16–18 April 2012
- Xia H, Wang D, Liu Z (2001) Study of the mechanism of polymer solution with visco-elastic behavior increasing microscopic oil displacement efficiency. *Acta Pet Sin* 22:60–65 (in Chinese)
- Xia HF, Wang DM, Zhang JR (2012) Quantitative description of contribution of elasticity of polymer solution to oil displacement efficiency. *J China Univ Pet* 36:167–170
- Zaitoun A, Kohler N (1988) Two-phase flow through porous media: effect of an adsorbed polymer layer. In: Paper SPE 18085 presented at the 1988 SPE annual technical conference and exhibition, Houston, 2–5 Oct
- Zhang LJ, Yue XA (2007) Mechanism for viscoelastic polymer solution percolation through porous media. *J Hydrodyn* 19:241–248
- Zhang Z, Li JC, Zhou JF (2010) Microscopic roles of “viscoelasticity” in HPMA polymer flooding for EOR. *Transp Porous Med* 86:199–214
- Zhao XQ, Pan F, Guan WT (2011) A novel method of optimizing the molecular weight of polymer flooding. In: Proceedings of the SPE enhanced oil recovery conference, Lumpur, Malaysia, 19–21 July 2011
- Zhou SW, Han M, Xiang WT (2006) Research and application of polymer flooding in Bohai Bay oilfield. *China Offshore Oil Gas* 6:387–389
- Zitha P, Chauveteau G, Zaitoun A (1995) Permeability dependent propagation of polyacrylamides under near-wellbore flow conditions. In: Proceedings of the SPE international symposium on oilfield chemistry, San Antonio, TX, USA, 14–17 Feb 1995

Publisher's Note Springer Nature remains neutral with regard to jurisdictional claims in published maps and institutional affiliations.